Catalysis Today 140 (2009) 23–29

Contents lists available at ScienceDirect

Catalysis Today

journal homepage: www.elsevier.com/locate/cattod

The use of mesoporous molecular sieves containing niobium for the synthesis of vegetable oil-based products

Agnieszka Feliczak, Katarzyna Walczak, Agata Wawrzyńczak, Izabela Nowak *

Faculty of Chemistry, Adam Mickiewicz University, Grunwaldzka 6, PL-60-780 Poznan, Poland

ARTICLE INFO

Article history:
Available online 10 September 2008

Keywords:
Organosilicas containing niobium
Characterization
Stability
Oxidation activity
Renewables
Sunflower oil

ABSTRACT

A synthetic protocol for the preparation of periodic mesoporous organosilicas containing niobium (Nb-PMOs) is presented. The nanostructured bridged organoniobosilicates have been synthesized by the acid catalyzed hydrolysis and condensation of bridged silsesquioxane precursors containing two different organic bridging groups ($(C_2H_5O)_3Si–R–Si(OC_2H_5)_3$, R: ethylene or octylene) in the presence of nonionic template P123. The retention of niobium and organic groups in the organosilica framework was ensured by slow template removal. A successful synthesis of Nb-PMOs was confirmed by powder X-ray diffraction (high periodicity), N_2 adsorption (surface area about 900 $m^2\ g^{-1}$ and narrow pore size distribution with maximum at about 4–11 nm), transmission electron microscopy (hexagonal symmetry), diffuse reflectance UV–visible spectroscopy (characteristic absorption band for Nb in the framework), H_2-temperature-programmed reduction (localization of Nb in the framework) and FTIR spectroscopy (presence of CH_2–$Si(OSi\equiv)_3$ groups). Experiments show that increasing the content of the organic chain length functionality in the precursors is found to significantly worsen the mesostructural ordering of the product. It is shown that the niobium can act as a co-template in making nanoporous organosilica materials.

The presence of niobium species neighboring with organic bridges in Nb-PMOs offers new prospects for application of these materials in catalysis. These niobosilicate materials showed excellent catalytic activity and selectivity for direct oxidation of vegetable oil ingredients into valuable products under mild liquid phase conditions using dilute H_2O_2 as an oxidant.

1. Introduction

Since the advent of high-surface area mesoporous molecular sieves (e.g., M41S-type silica materials) via a surfactant-templated synthesis route by Mobil in 1992 [1], organic modification schemes imparting various functionalities to the inorganic silica surface have received much attention. By using a bistrialkoxysilyl precursor in which bonding between silicon and carbon is established with the assured stoichiometry, periodic ordered mesoporous organosilicas (PMOs) materials in which organic groups have been directly integrated into silica framework were synthesized in 1999 by three independently working groups [2–4]. These new materials have been expected to lead to advanced materials due to the possibility of controlling the kind of functional groups in the bridged organosilane precursors ($(R'O)_3–Si–R–Si–(OR')_3$, e.g. [5]). Till date, PMOs with simple bridging groups derived from methane, ethane, ethylene, acetylene, phenyl, and its derivatives, thiophene, and ferrocene have been developed (e.g., review paper [6]). The pore diameters of the PMOs prepared by structure-directing agents with ionic alkyl ammonium surfactants (with chain lengths from C12 to C20) were restricted to the range between 2 and 5 nm. This limitation was finally overcame by using nonionic triblock copolymers such as P123 ($EO_{20}PO_{70}EO_{20}$) that was used previously as a structure directing agent in the synthesis of large-pore mesoporous SBA-15 pure silica phase. This kind of material with a hexagonal *P6mm*-type structure is the representative of 2D mesostructure and possesses wall thicknesses between 3.1 and 6.4 nm with pore sizes in the range of 4.6–30 nm [7].

The PMOs materials have gained the general expectation that their efficient uses can be dimensionally expanded to a number of versatile applications as catalysts. Hence, intellectual efforts are subsequently devoted to extend the unique properties of the PMO in the area of heterogeneous catalysis, by the substitution of active metal sites in the wall positions so that they can be used as catalyst for various hydrophobic reactions, e.g. (ep)oxidation processes in order to improve the contact at the water (oxidant)–organic interface [8]. Since the Nb-containing silicas were found to be active in oxidation processes [9], in this work we synthesized and optimized the synthesis condition of the new Nb-PMOs catalysts that are expected to find applications as water-tolerant solid acid

* Corresponding author. Tel.: +48 61 829120; fax: +48 61 829120.
E-mail address: nowakiza@amu.edu.pl (I. Nowak).

0920-5861/$ – see front matter © 2008 Elsevier B.V. All rights reserved.
doi:10.1016/j.cattod.2008.07.012

catalysts for the reactions that require weak acidic sites and low temperatures. Periodic mesoporous organosilicas (PMOs) with (–CH_2–) bridges and different amounts of niobium have been synthesized via one-step synthesis. Especially, porous materials with a well-defined pore geometry are desirable as catalysts and adsorbents for highly selective reactions.

The application of vegetable oils in the chemical industry is becoming more and more significant because of their accessibility from renewable resources. Epoxidized vegetable oils play an important role as building blocks for the preparation of chemical intermediates that are the basis for a wide variety of consumer products [10]. Especially, they can be used as plasticizers and stabilizers, reactive diluents for paints, intermediates in the production of polyurethane–polyols, as well as components of lubricants and adhesives [11]. The catalytic epoxidation of oleochemicals has been the subject of many academic and industrial investigations (e.g. [12,13]). As the renewable raw materials are going to play a very noteworthy role in the development of sustainable green chemistry, thus it is necessary to replace the only commercial source of epoxidized oils, i.e., the Prileshajev reaction, which uses short chain percarboxylic acids [14]. Especially, the major drawback of these catalysts is that they are non-regenerable, corrosive and must be used in more than stoichiometric amount. From these reasons, the development of new type of acid catalysts, especially heterogeneous ones, is rather challenging. A steady increase in the use of eco-friendly consumer products like lubricants has occurred as a result of strict government regulations and increased public awareness for a pollution-free environment [15]. Oils and fats of vegetable and animal origin share the greatest proportion of the current consumption of renewable raw materials in chemical industry [16].

Since the Nb-containing organosilicas are expected to find applications as water-tolerant solid acid catalysts for the reactions that require weak acidic sites and low temperatures, in this work we tested for the first time the Nb-PMOs catalysts in vegetable oil oxidation reactions, i.e., eco-friendly liquid oxidation with dilute hydrogen peroxide. Moreover in the present study, we addressed the question of whether mesoporous materials; i.e., OMS (ordered mesoporous silicas) and PMOs may be involved not only in the primary epoxidation reactions but also in the subsequent oxidation steps leading to the formation of long-chain dioic acids, which are then subjected to peroxisomal β-oxidation into acetyl coenzyme A.

2. Experimental

2.1. Catalysts preparation

The triblock copolymer Pluronic P123 ($EO_{20}PO_{70}EO_{20}$) was obtained from BASF, while 1,2-bis(triethoxysilyl)ethane (BTEE) and 1,8-bis(triethoxy-silyl)octane (BTEO) were provided by ABCR GmbH & Co. In a typical synthesis, the P123–H_2O solution was slowly added to the BTEE (or BTEO)–Nb source–H_2O–HCl mixture that was stirred for 24 h at 313 K. The slurry was then transferred into a polypropylene bottle and autoclaved at 373 K for 120 h. The white solids were recovered by filtration, washed with deionized water and ethanol, and dried under ambient conditions. For all as-synthesized materials, the surfactant molecules were removed by solvent extraction (mixture of ethanol and HCl). The samples will be denoted as Nb(R)-PMO-E in the case of using BTEE and Nb(R)-PMO-O for BTEO, respectively, where R = Si/Nb ratio (R = 16, 32, 64).

2.2. Materials characterization

The materials were characterized by X-ray diffraction (XRD), transmission electron microscopy (TEM), adsorption measurements, DTG/TG, UV–vis and FTIR spectroscopies and H_2-TPR study. They were tested in the liquid phase oxidation with H_2O_2 as an oxidant.

Si and Nb contents were determined by X-ray fluorescence, i.e. XRF (MiniPal, Philips) using calibration curves prepared from mixtures of mesoporous pure organosilica and niobia.

Samples for TEM were prepared by the grinding of the powder and successive ultrasonic treatment in isopropyl alcohol for 1 min. A drop of the suspension was dried on the standard TEM sample grid covered with holey carbon film. JEOL 2000 electron microscope operating at 80 kV was used for observations.

The XRD patterns of the powder materials were recorded by a TUR-62 diffractometer using a Ni-filtered Cu (Kα) radiation operating at 40 kV and 30 mA. The 2θ range started from 1.4° and with a step of 0.02°. The $h\,k\,l$ indexes of materials were calculated based on the Bragg diffraction equation.

Micromeritics 2010 was used to measure the nitrogen adsorption/desorption isotherms of the catalysts. Prior to the measurements, the materials were outgassed at 573 K for 3 h. The BET specific surface area was calculated using BET equation in the range of relative pressure between 0.05 and 0.25. The KJS–BJH method was used to calculate the pore volume and the pore size distribution with the use of the adsorption branch of the isotherm [17]. Moreover, α_s-plot analysis was performed for all obtained samples for the purpose of the evaluation of microporosity.

Ultraviolet and visible-light diffuse reflection (UV–vis-DR) spectra were recorded on a doubled beam Varian Carry 300 spectrophotometer using Praying Mantis DR attachment. The spectra were recorded against a Labsphere certified reflectance standard (99.9%) for solid samples in the range of 900–190 nm. The DR spectra were recalculated with the Kubelka–Munk equation in the limit of infinite thickness (denoted $F(R)$).

To evaluate the reducibility of Nb species in the samples, H_2-temperature-programmed reduction (H_2-TPR) was conducted, using a TPR apparatus (Micromeritics 2705). A sample (0.04 g) was pretreated in a He flow at 723 K for 1 h and then cooled to room temperature. Lastly, the reduction of the sample was carried out in an H_2/Ar (10 vol.%) flow of 40 $cm^3\,min^{-1}$ from room temperature up to 1373 K with a ramp of 10 K min^{-1}. Outlet H_2 concentration was monitored continuously using a TCD, which allowed the evaluation of H_2 consumption.

Thermal analyses—thermogravimetry was performed on a TG Setaram SetSys12 thermobalance in air or nitrogen flow with an ~11 mg sample. The heating rate was 10 K min^{-1} (temperature range: 303–1103 K).

2.3. Catalytic testing

The catalytic performance of the materials was tested in three oxidation reactions: epoxidation of methyl oleate or fatty acid methyl ester (FAME) mixture and oxidation of C18 fatty acid. In the epoxidation reaction case, the methyl oleate and FAME mixture were obtained from oleic acid and sunflower oil, respectively, by esterification with $NaOCH_3$ and followed by distillation. The composition of FAME mixture was determined by GC–MS and it consists of the following methyl esters: oleate (79%), linoleate (12%), stearate (6%), palmitate (3%) and behenate (traces). The epoxidation tests were carried out under inert atmosphere in a glass batch reactor at 343 K using hexane as solvent (10 cm^3; Riedel de Haen; solvent: substrate volume ratio = 8), hydrogen peroxide as oxidant (oxidant: substrate molar ratio = 1), ca. 0.30 cm^3 of FAME mixture and 40 mg of solid catalyst. Samples were taken after a reaction time of 1, 3, 6 and 24 h and analyzed by GC. The final product identification was done by GC–(EEI)MS–MS. The analysis was performed with a Varian GC3800 gas chromatograph coupled with a

Varian 4000 ion trap mass spectrometer. Samples were injected in the split mode and run on a capillary column (VF-5MS (Varian) with following parameters: 30 m long, 0.25 mm internal diameter; 0.25 μm coating thickness of 95% dimethylsiloxane cross-linked with 5% phenylmethylsiloxane). The oven temperature was programmed for 2 min at 373 K and then increased linearly to 573 K at a rate of 8 K min^{-1}. The carrier gas was helium. A similarly equipped Varian GC3800 gas chromatograph using helium as the carrier gas and a flame ionization detector (however, with slightly different VF-5MS column: 0.5 μm coating thickness, 30 m long and 0.53 mm diameter) was used for product quantification, with the help of calibration curves.

The third catalytic reaction, oxidation of stearic acid, was done in similar way.

3. Results and discussion

Highly ordered mesoporous organoniobosilicates with large pores were synthesized for the first time under acidic conditions using Pluronic 123 triblock copolymer as a supramolecular structure directing agent. Ethane- and octane-bridged Nb-PMOs were prepared by co-condensation using BTEE and BTEO, respectively in the presence of triblock copolymer. Table 1 summarizes the structural properties of the Nb-substituted and bridging organic groups containing mesoporous molecular sieves. XRF analysis showed that the molar ratio of silicon to niobium in the final product was higher than in the synthesis mixture (see Table 1). The use of the bistriethoxysilane precursors in the synthesis procedure for the preparation of Nb-PMOs materials led to about four times lower amount of niobium incorporated in comparison to about twice lower amount in the case of sample without organic groups. Under the synthesis conditions used in this work, only a part of niobium (25%) was incorporated into the final mesoporous material due to the strong acidic conditions during the synthesis procedure and the competition between niobium species and bridging organic groups.

The mesostructural ordering of the as-synthesized and extracted Nb-PMOs was confirmed by powder XRD. The low-angle XRD patterns of Nb-PMOs treated under different conditions are shown in Fig. 1 and all display the main reflection peak at ca. $2\theta = 0.5–1.5$, that can be indexed to the (1 0 0) diffraction line. Similarly to pure niobosilicate analogues (i.e., NbSBA-15), Nb-PMOs without extraction exhibit XRD patterns dominated by low-angle peaks, typically with a prominent peak with a d spacing ($d_{1\,0\,0}$) of ~13 nm (see Fig. 1, line a). The XRD pattern indicates a significant level of mesostructural ordering [18]; however, there is a lack of higher order peaks. This is a known feature of XRD patterns of template-containing mesophases. The XRD pattern of the extracted nioboorganosilicate Nb-PMO-E exhibits a high intensity prominent (1 0 0) peak along with (1 1 0) and (2 0 0) peaks, and therefore confirmed that the mesophase has hexagonal (*P6mm* symmetry group) pore channel ordering. The material obtained from the silica source containing longer bridging carbon chain (Nb-PMO-O; not shown here) showed the characteristic peaks at low angle, however they were less resolved. Similarly to pure niobosilicate counterparts, Nb-PMOs exhibit XRD patterns dominated by low-angle peaks, typically with a prominent peak at $2\theta < 1.6^\circ$. After calcination, a decrease in $d_{1\,0\,0}$ peak intensity, long-range ordering and lattice contraction (see the next paragraph) of this observed (Fig. 1, line c), showing the cross-linking of the framework silanols and/or the lack of ordering between the structures of adjacent pores. In addition to the structural ordering, XRF analysis showed that the hydrophobic nature of surfactant also plays a vital role in the amount of metal incorporation (Table 1). Even though there is no stoichiometric incorporation of niobium under the present synthesis conditions, it is likely that a large part of the metal remains in the gel solution.

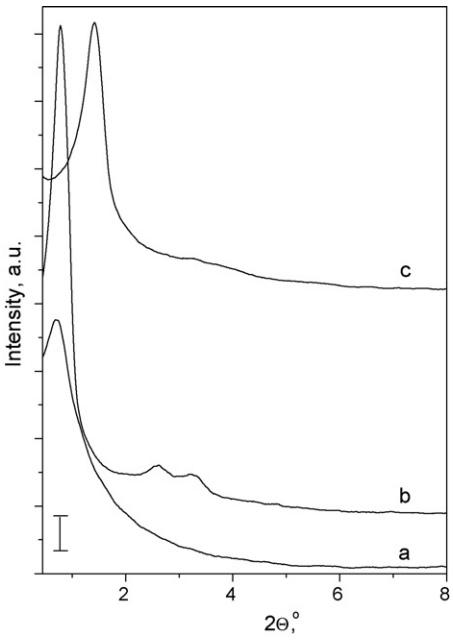

Fig. 1. XRD patterns for the Nb-PMO-E samples: (a) as-synthesized; (b) after extraction with HCl/EtOH mixture; (c) after extraction and calcination at 773 K for 4 h.

The structure of all the extracted NbPMOs was studied by X-ray diffraction and XRD patterns were typical for two-dimensional hexagonal structure as it is illustrated in Scheme 1. The $d_{1\,0\,0}$ spacings are tabulated in Table 1. The incorporation of Nb into the framework of PMOs is evidenced by an increase in the d spacings of

Table 1
Textural and structural properties of Nb-PMOs materials and their niobosilica analogue*

Material	Si/Nb	$d_{1\,0\,0}$	Surface area ($m^2\,g^{-1}$)	Pore width (nm)	Pore volume ($cm^3\,g^{-1}$)				Wall thickness (nm)
					Total	Meso	Micro	Textural	
Nb(16)-PMO-E	81	12.0	940	8.5	1.19	0.93	0.12	0.14	3.5
Nb(32)-PMO-E	123	13.0	820	9.8	1.12	0.92	0.08	0.12	3.2
Nb(64)-PMO-E	243	13.6	720	10.6	1.05	0.93	0.03	0.09	3.0
PMO-O	–	–	20	~2.8	0.04	0.03	0.00	0.01	–
Nb(16)-PMO-O	67	8.5	400	~4.0	0.74	0.49	0.00	0.25	4.5
Nb(32)-PMO-O	121	8.8	350	~5.0	0.62	0.47	0.00	0.15	3.8
Nb(64)-PMO-O	238	9.5	320	~6.0	0.51	0.43	0.00	0.08	3.5
Nb(64)SBA-15**	156	12.9	900	10.3	1.07	0.89	0.13	0.05	2.3

*Wall thickness: a_0 ($a_0 = 2d_{1\,0\,0}3^{-1/2}$) − (pore width); volume of textural mesopores was obtained as the difference between total pore volume ($p/p_0 = 0.99$) and the sum of micro- and mesopore volumes (α_s-plot); pore size analysis was performed by the KJS method. **Synthesized with TEOS as a Si source.

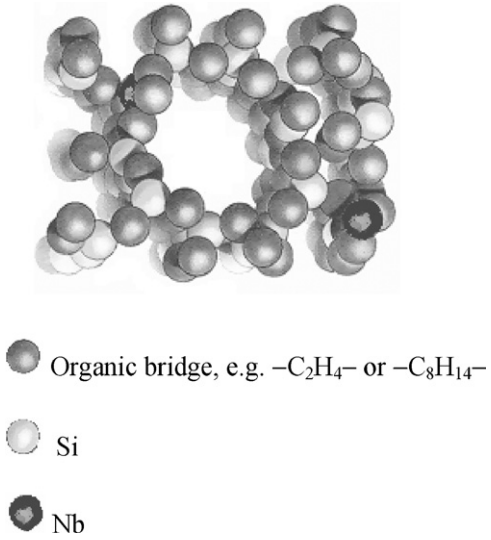

Scheme 1. General idea of Nb-PMOs materials. Oxygen atoms are not drawn to make this picture clearer.

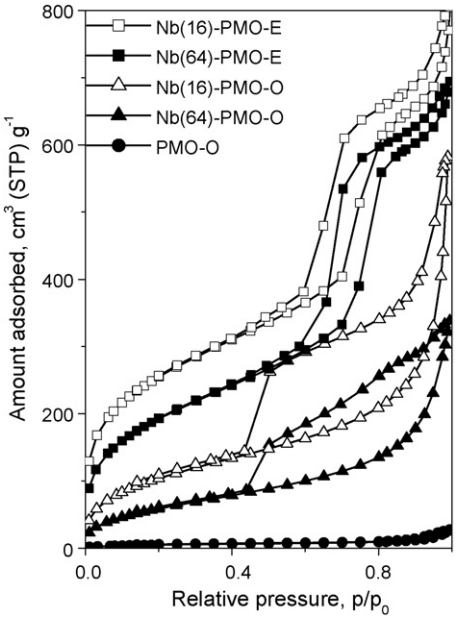

Fig. 3. Nitrogen adsorption–desorption isotherms at 77 K for Nb-PMOs materials.

Nb-PMO samples, suggesting a more thinned framework in the Nb-PMO samples. Moreover, it is also interesting to note that the $d_{1\,0\,0}$ spacing parameter decreased in the following way: Nb-PMO-O < Nb-PMO-E that confirms the strong influence of organic spacer on the mesochannels system. The (1 0 0) interplanar spacings for hydrothermally treated samples tended to be slightly lower than those observed for extracted samples.

The TEM images (Fig. 2) recorded for the samples prepared with ethylene and octylene bridging groups prove that the hexagonal structure was formed. This behavior was not dependent on the niobium content. For the samples prepared with octylene bridging groups, more irregularly shaped pores were observed, that is reflected by a wormlike structure.

In addition to the XRD and TEM, gas adsorption was a technique of supplementary choice for the evaluation of pore size distribution, pore volume, and surface area of these materials [19,20]. The textural features were typical of mesoporous materials and are varied depending on the niobium content and organic spacer. Surface areas, pore sizes and pore volumes of the PMO materials are tabulated in Table 1. The synthesis afforded Nb-PMO-E materials with pore sizes between 8 and 11 nm and specific surface areas in the range of 700–900 $m^2\,g^{-1}$. The isotherms of PMO-E samples are of type IV with a pronounced uptake in the relative pressure range of 0.7–0.9 due to capillary condensation in the mesopores, indicating the presence of relatively uniform mesopores (Fig. 3). A visible increase in adsorption at $p/p_0 > 0.9$ associated with hysteresis for NbPMOs could be attributed to the existence of interparticle pores. The isotherms of PMO-O samples are between types I and IV, which is furthermore evidenced by the presence of small pore diameter (2.8 nm). In addition, the shift of the mesopore filling step to the lower relative pressure with the niobium incorporation indicates that the pore diameter of Nb-PMO is smaller than that of PMO, as confirmed by the data in Table 1. A gradual increase in the micropore volume is observed after introduction of niobium to the synthesis gel. This is also accompanied by an increase in the primary and textural (secondary) mesopore volumes, while the wall thickness changes in opposite way (Table 1).

The thermogravimetric analysis (TGA) under nitrogen atmosphere for as-synthesized Nb-PMO samples (not shown here) showed a weight loss below 373 K related to the removal of physisorbed water. A subsequent large weight loss (up to 31%) observed between 373 and 623 K can be assigned mostly to surfactant decomposition. The partial loss of organic groups at 623 K was observed with complete removal of ethane groups by 873 K and octane groups by 923 K. Thus one can conclude that at temperatures above 623 K a significant weight loss that is largely

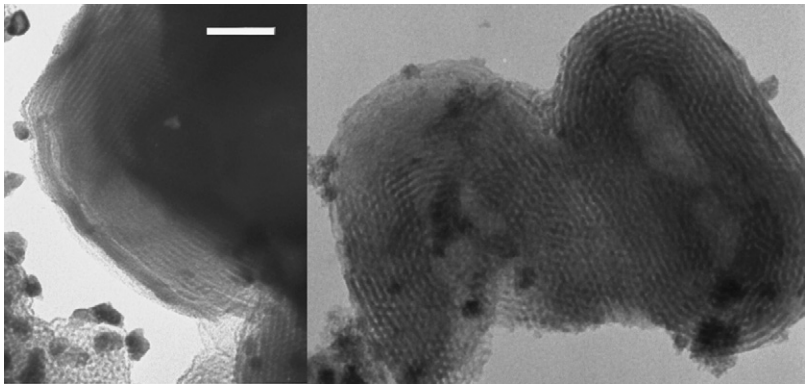

Fig. 2. Transmission electron micrographs for Nb-PMO-E. The bar represents 100 nm.

completed at about 900 K took place, which is attributable to the removal of the organics from the material.

The FTIR spectra of the template-removed PMO exhibited (not shown here) bands at 2930 cm^{-1} (asymmetric C–H stretching vibration of $–CH_2–$ fragments), 2860^{-1} (symmetric C–H stretching vibration of $–CH_2–$ fragments), 1170 cm^{-1} ($Si–CH_2–CH_2–Si$ stretching mode), 1410 and 1270 cm^{-1} (CH_2 deformation vibrations), as well as 696 and 768 cm^{-1} (Si–C stretching modes), which are consistent with those observed in the literature for hydrocarbon-bridged PMO materials (e.g. [21]), showing their successful synthesis. Furthermore, the Raman data provided a strong evidence that the template was completely removed via extraction and the Si–C bond was formed during synthesis and was not altered during extraction stages.

Important information relevant to the discussion of the location of niobium in PMO-type materials is provided by the few techniques, e.g., wide-angle X-ray diffraction, UV–vis spectroscopy and H_2-TPR. The first technique can be useful for the identification of oxide-type crystalline phases present in the matrix (the so-called extra framework species), however the recorded diffractograms did not indicate the presence of characteristic signals due to crystalline Nb oxides phases, which can be also connected with the low niobium content.

Diffuse reflectance UV–vis spectroscopy is a very sensitive probe for the presence of extra-framework heteroatoms in molecular sieves. Thus, the localization of niobium species was further elaborated using this kind of spectroscopy. The presence of a band at 225 nm on the UV–vis patterns for Nb-PMOs (Fig. 4) clearly indicates a successful incorporation of niobium into the framework (matrix). No bands typical for five- and six-coordinated Nb species (~250 nm) in small niobia nanodomains species [22] were observed in the spectra. The absence of peaks above 300 nm for the prepared samples indicates that no bulk niobia is formed.

The H_2-TPR study (Fig. 5) reveals that the NbPMOs materials possess mainly niobium reduced at very high temperatures, most probably incorporated to the framework (matrix) of silica sieves. It is known [23] that the low temperature (LT) peaks (below 1000 K)

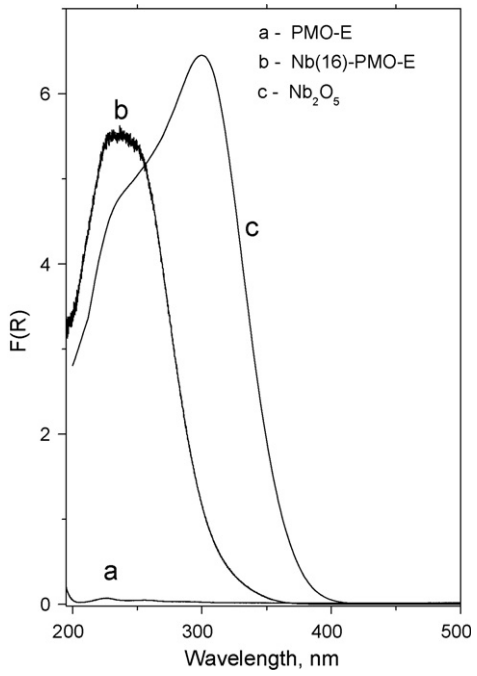

Fig. 4. UV–vis spectra for Nb(16)-PMO-E (b) and bulk Nb_2O_5 (c) together with pure organosilicas analogue (a).

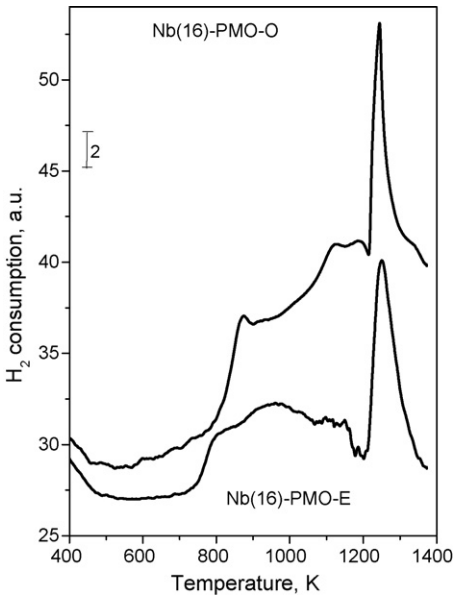

Fig. 5. The H_2-TPR profiles for Nb(16)-PMO-O and Nb(16)-PMO-E materials.

are due to the reduction of extra-framework niobium species, whereas, those at high temperatures (HT) – above 1000 K – characterize the reduction of niobium localized in the framework. Thus, the peak at 1350 K can be assigned to Nb^+ species connected with the silica tetrahedra [23]. It is worthy to stress that in the case of sample prepared with the use of a small amount of niobium (Si/Nb = 64, not shown here) the at 1350 K was less intensive and its intensity gradually increases with the increase of niobium concentration in the synthesis mixture.

The catalytic results obtained for different solids (also with niobium catalyst having similar loading but without organic bridging groups) are gathered in Tables 2 and 3. Prior to the experiments a possibility of homogeneous catalysis over niobium-containing solutions and of niobium leaching were taken into accounts. This question was answered by performing special experiments previously for cyclohexene oxidation [24] and by additional experiments. The oxidation of FAME and methyl oleate was carried out in the homogeneous phase over the same amounts of niobium precursor (as that used for the synthesis of Nb-PMOs catalysts) in hexane. Moreover, the reaction carried out in the solution obtained by H_2O_2 treatment on the catalysts showed only residual activity after admission of reagents. In both cases, very low activity (<1–3%) were registered. Additionally, there was almost no activity, when the sample was first stirred with reagents for 4 h and later, after removal of the catalyst, the reaction was carried out in the solution after addition of hydrogen peroxide. Moreover, the reaction ran on pure silica PMO sample showed almost no activity in the oxidation of methyl oleate and FAME.

Nb-PMOs were tested in oxidation of methyl oleate under mild conditions (diluted hydrogen peroxide, 343 K). Epoxyderivative of methyl oleate – 9,10-epoxyoctadecanoic acid methyl ester – was obtained as the only product, with no traces of 9,10-dihydroxyoctadecanoic acid methyl esters or other products (e.g., due to oxidative cleavage of the C=C double bond or to diol cleavage). In addition, the reaction was stereospecific: only the *cis*-epoxide was formed. Fig. 6 shows the time conversion plots for two different catalysts, namely Nb-PMO-E. As expected, the conversion increases directly with the niobium content, however there is no linear correlation between these two factors. The methyl oleate was almost totally epoxidized after 24 h; while the conversion of

Table 2
Epoxidation of methyl oleate and sunflower oil using different nioboorganosilicas and niobosilica

Catalysts[a]	Methyl oleate (%)		Sunflower oil (%)		
	Conversion	Epoxide selectivity	Conversion	Selectivity	
				Monoepoxy-derivative	Diepoxy-derivative
Nb(16)-PMO-E (81)	99	100	95	75	9
Nb(32)-PMO-E (123)	95	100	92	72	10
Nb(64)-PMO-E (243)	91	100	87	70	12
Nb(16)-PMO-O (67)	99	100	96	79	1
Nb(32)-PMO-O (121)	93	100	92	77	2
Nb(64)-PMO-O (238)	89	100	88	70	4
Nb(64)SBA-15 (156)	69	81	66	65	14

Conditions: aqueous H_2O_2/substrate = 1 (mmol/mmol); substrate/catalyst = 8 (v/v); 343 K, 24 h.
[a] The last two numbers in brackets denotes the real Si/Nb ratio.

Table 3
Oxidation of stearic acid using different nioboorganosilicas and niobosilica

Catalysts*	Conversion (%)	Selectivity (%)		
		ω-hydroxy acid	Dicarboxylic acid	Others**
Nb(16)-PMO-E (81)	97	75	15	10
Nb(32)-PMO-E (123)	95	77	13	10
Nb(64)-PMO-E (243)	93	78	12	10
Nb(16)-PMO-O (67)	99	82	12	6
Nb(32)-PMO-O (121)	93	86	11	3
Nb(64)-PMO-O (238)	95	88	11	1
Nb(64)SBA-15 (156)	66	25	5	70

Conditions: aqueous H_2O_2/stearic acid = 1 (mmol/mmol); stearic acid/catalyst = 8 (v/v); 343 K, 24 h. *The last two numbers in brackets denotes the real Si/Nb ratio; **e.g., peruvic and azelaic acids due to oxidative cleavage.

methyl oleate was slightly lower after 6 h (Fig. 6, left side). The selectivity for epoxide was better than 99% in each case. The conversion for the niobium-containing materials in the epoxidation reaction after 24 h decreases in the following order: Nb(16)-PMO > Nb(32)-PMO > Nb(64)-PMO and follows the same order for both bridging organic groups. The different reactivity for different organic spacing group can be explained by the various surface areas and proper mesoporous ordering of the synthesized nioboorganosilicates.

The influence of calcination (i.e., removal of the organic spacer) on the reaction had been investigated. The reactivity change profile (i.e., decrease from ~90% to ~70%) in each case indicated that the presence of organic groups seemed to be crucial for the generation

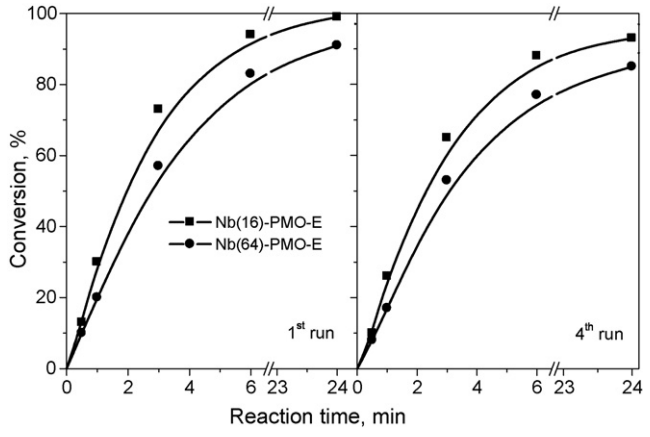

Fig. 6. Conversions in the epoxidation of methyl oleate with Nb-PMOs in the first and fourth run.

of catalytic activity on the composite. It is worthy to stress that the pure niobosilicate (Nb-SBA-15) prepared with a use of tetraethoxy ortosilicate instead of bistriethoxysilane precursors showed similar conversion to the calcined sample. In our previous paper [24], the reactivity of NbSBA-15 samples in the epoxidation of cyclohexene was compared to the behavior of other mesoporous materials containing niobium. It was concluded that the epoxide formation strongly depends on niobium isolation in the matrix and thus on the oxidative surface properties. Especially in the presence of acid centers epoxide can react further with another molecule of hydrogen peroxide or water to form a diol. The incorporation of organic groups in our case causes the proper isolation of niobium in NbPMOs and gives the proper balance between acidic and redox (oxidative) properties. The acidic and oxidative properties as well as hydrophobic character of the surface (toluene/water adsorption) are currently under deeper investigation.

The TON value (total number of product molecules formed per active site) calculated at 24 h of reaction time (epoxidation of methyl oleate) was 720 molecules/Nb site for Nb(64)-PMO-O (Si/Nb ratio of 238) and about 200 molecules/Nb site for Nb(16)-PMO-O (Si/Nb = 67). These values were calculated assuming that all Nb^{5+} species are located on the surface, however the presented data clearly shows that the TON calculations are not accurate for mesoporous materials, where most of metal sites (species) are located deeper insides walls and thus are inaccessible for reagents. It is worthy to stress that the wall thickness (Table 1) was thicker for lower Si/Nb ratio, i.e., for higher niobium content. Another features, i.e., additional porosity – the textural mesoporosity (secondary mesopores) and microporosity – were also superior for very low Si/Nb ratio and this features can be connected with higher methyl oleate conversions.

The recycling of the catalyst was evaluated for four cycles for all the Nb-PMO catalysts. In these experiments, the catalysts were filtered after each step. With methyl oleate, the nioboorganosilicates were used four times with small loss in conversion efficiency and no significant changes on the selectivity (example in Fig. 6). However, such decrease can be explained by the loss of the catalyst during the filtration procedure.

The activity in the epoxidation of methyl esters of sunflower oil, which major component is methyl oleate (79%), was found to be slightly higher for Nb-PMO-O than for Nb-PMO-E. After 24 h, the unsaturated FAMEs of the mixture were practically completely epoxidized over Nb(16)-PMO-O, whereas the conversion was slightly lower over other catalysts. The highest conversion of FAME and the selectivity for monoepoxide product were 99% and 79%, respectively. A high catalytic activity of niobium-doped PMOs is associated with the presence of hydrophobic environment around Nb species and their proper isolation. An increase in the carbon chain length of nonpolar organic bridge (organic spacer) enhances

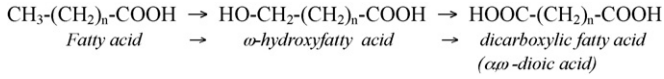

Scheme 2. Proposed scheme of the oxygenation cascade from fatty acids to α,ω-dioic acids.

hydrophobicity of the resulting Nb-PMO, and consequently increases the catalyst's selectivity. Moreover, it was found that depending on the niobium content, the resulting materials showed only slight differences in their catalytic performance in the liquid phase oxidation. The samples with low Si/Nb molar ratio were found to be the most active catalysts. Such new hydrophobic catalyst showed better performance (increase in the epoxide selectivity besides the catalytic conversion) when compared to the niobosilicate catalyst (Table 2). With regard to the selectivity, almost all the Nb-PMO catalysts led selectively to the formation of *cis*-9,10-epoxyoctadecanoic acid methyl ester (the monoepoxy-derivative of methyl oleate). The highest selectivity value was recorded over Nb-PMO-O (79% in respect to all sunflower oil components and 100% in respect to methyl oleate). On the contrary, higher selectivity to diepoxyderivative (*cis*-9,10; *cis*-12,13-bis epoxyoctadecanoic acid methyl ester) in addition to monoepoxyderivative was detected for Nb-PMO-E that can be connected with different niobium coordination in the presence of shorter organic bridging group (spacer).

The ability of NbPMO to efficiently catalyze an oxygenation cascade (stearic acid → ω-hydroxystearic acid → α,ω-octadecandioic acid path as depicted in Scheme 2) on a given fatty acid substrate provides new insights into the applicability of Nb-PMOs in the formation of vegetable oil-based valuable products. The catalytic results for the oxidation of stearic acid with the NbPMOs catalysts are presented in Table 3. The reactivity of these catalysts is in the order: Nb-PMO-O > Nb-PMO-E. This hierarchy is a function of the surface area and probably the niobium dispersion/isolation and follows the same order as the epoxidation of methyl oleate and FAME. The formation of subsequent oxygen-rich compounds is dependent on the presence of oxygen donor (i.e., H_2O_2), thus under the applied conditions (aqueous H_2O_2/stearic acid = 1 (mmol/mmol)) the reaction proceed first to (-hydroxystearic acid and then via a hydroxylation of the $-CH_2OH$ group to α,ω-octadecandioic acid. To conclude, new catalysts allowed by-passing in producing ω-hydroxyfatty acids and/or dicarboxylic acids (α,ω-dioic acid) for β-oxidation purposes (i.e., transformation of fatty acid into acetyl coenzyme A). The influence of the reaction conditions on the catalytic performance of NbPMOs materials is currently under investigation.

4. Conclusions

A new ordered mesoporous hybrid material with ethane- and octane-niobosilica framework, where organic and inorganic moieties are distributed homogeneously at the molecular level in the framework, has been synthesized. The periodic mesoporous material consistent of nioboorganosilicate is stable after surfactant removal up to almost 900 K. Several characterization techniques (XRD, TEM and N_2 adsorption–desorption studies) corroborate the mesoporous texture/structure. The XRD patterns were supported by the hexagonal symmetry, while TEM is also strongly supporting the XRD patterns. The UV–vis spectra indicated the successful incorporation of niobium into hybrid mesoporous materials, which was also supported by H_2-TPR data. The surface area and pore diameter were reduced with increasing loading of niobium. Testing of the hybrid material as a catalyst demonstrated a promising result, which closely approaches the performance of a potential commercial product. The activity followed the same trend as in the case of the sunflower oil oxidation reaction.

Acknowledgements

The generous donation of BTEE and BTEO from ABCR and Pluronic P123 from BASF (BTC-Benelux and BASF-Poland) and financial support from Polish Ministry of Scientific Research and Information Technology (grant N204 084 31/1965; 2006–2009) are gratefully acknowledged. The Foundation for Polish Science is accredited for granting the acquisition of the GC–MS–MS detector (Novum Programme, Support for the Development of Research Facilities; grant no. 9/2007).

References

[1] C.T. Kresge, M.E. Leonowicz, W.J. Roth, J.C. Vartuli, J.S. Beck, Nature 359 (1992) 710.
[2] S. Inagaki, S. Guan, Y. Fukushima, T. Ohsuna, O. Terasaki, J. Am. Chem. Soc. 121 (1999) 9611.
[3] T. Asefa, M.J. MacLachan, N. Coombs, G.A. Ozin, Nature 402 (1999) 867.
[4] B.J. Melde, B.T. Holland, F. Blanford, A. Stein, Chem. Mater. 11 (1999) 3302.
[5] T. Asefa, M. Kruk, M.J. MacLachan, N. Coombs, H. Grondey, M. Jaroniec, G.A. Ozin, J. Am. Chem. Soc. 123 (2001) 8520.
[6] F. Hoffmann, M. Cornelius, J. Morell, M. Froba, Angew. Chem. Int. Ed. 45 (2006) 3216.
[7] D. Zhao, Q. Huo, J. Feng, B.F. Chmelka, G.D. Stucky, J. Am. Chem. Soc. 120 (1998) 6024.
[8] F. Fajula, A. Galarneau, F. Di Renzo, Micropor. Mesopor. Mater. 82 (2005) 227.
[9] I. Nowak, B. Kilos, M. Ziolek, A. Lewandowska, Catal. Today 78 (2003) 487.
[10] U. Biermann, W. Friedt, S. Lang, W. Luhs, G. Machmuller, J.O. Metzger, M.R. Klaas, H.J. Schafer, M.P. Schneider, Angew. Chem. Int. Ed. 3 (2000) 2206.
[11] F.D. Gunstone, in: F.D. Gunstone, F.B. Padley (Eds.), Lipid Technologies and Applications, Marcel Dekker, New York, 1997, p. 759.
[12] L.A. Rios, P. Weckes, H. Schuster, W.F. Hoelderich, J. Catal. 232 (2005) 19; R.E. Harry-O'kuru, S.H. Gordon, A. Biswas, J. Am. Oil Chem. Soc. 82 (2005) 207.
[13] Z.S. Petrovic, A. Zlatanic, C.C. Lava, S. Sinadinovic-Fiser, Eur. J. Lipid Sci. Technol. 104 (2002) 293.
[14] J.B. Williams, Eur. J. Lipid. Sci. Technol. 104 (2002) 361.
[15] U. Thiyam, A. Kuhlmann, H. Stöckmann, K.C.R. Schwarz, Chimie 7 (2004) 611.
[16] I. Rhee, NLGI Spokesman 60 (1996) 28.
[17] M. Kruk, M. Jaroniec, A. Sayari, Langmuir 13 (1997) 6267.
[18] S. Inagaki, S. Guan, T. Ohsuna, O. Terasaki, Nature 416 (2000) 304.
[19] J.M. Thomas, O. Terasaki, P.L. Gai, W. Zhou, J. Gonzalez-Calbet, Acc. Chem. Res. 34 (2001) 583.
[20] M. Kruk, M. Jaroniec, Chem. Mater. 13 (2001) 3169.
[21] U. Diaz-Morales, G. Bellussi, A. Carati, R. Millini, W. O'Neil Parker, C. Rizzo, Micropor. Mesopor. Mater. 87 (2005) 185.
[22] X.T. Gao, I.E. Wachs, M.S. Wong, J.Y. Ying, J. Catal. 203 (2001) 18.
[23] M. Ziolek, I. Sobczak, A. Lewandowska, I. Nowak, P. Decyk, M. Renn, B. Jankowska, Catal. Today 70 (2001) 169.
[24] I. Nowak, M. Ziolek, Micropor. Mesopor. Mater. 78 (2005) 281.